International Journal of Manufacturing and Material Processing
Vol. 2: Issue 1
www.journalspub.com

Effect of Cutting Parameters in Hard Turning on Chip Formation and Machined Surface

S. Choubisa, B.P. Nandawana, M.A. Saloda, M.S. Khidiya*
Department of Mechanical Engineering, College of Technology and Engineering, Udaipur, Rajasthan, India

Abstract

Cost effectiveness, increasing demand, high production rates and reliability of the product have increased the potential of industrial application of hard turning technology during the past few years. Grinding operation for hard steel component reduces the machining sequence, the machining time and the specific cutting energy. Hard turning also shows effects like generation of high temperature, the formation of saw toothed chips. In this thesis, experimental investigation is conducted in order to study the chip transition using Scanning Electron Microscopy and chip micro-hardness were conducted to correlate the chip morphology, cutting forces using micro-hardness tester. The surface integrity of machines part is also investigated. This study focuses on surface and sub-surface defects and white layer formation. The machined surfaces are examined using SEM to study effect of different process parameters on the quality of the machined surface. Cutting forces were measured by lathe tool dynamometer and ANOVA test were performed to observe the effect of cutting parameters on cutting forces.

Keywords: AISI D2 steel, chip formation, cutting forces, hard turning, microstructure of machined surface ANOVA

****Corresponding Author***
E-mail: choubisa.shambhu@gmail.com

INTRODUCTION

For aerospace industries high precision hardened steel is required therefore hard turning technology has been increased and now a dayshard turning has been replaced the grinding processes of hardened steel components in practice. Improved ceramic tool and CBN tool have been emerged as very important cutting for machining of hardened steel without any coolant. If we talk economically then it also provides less –effective time, less cost and most importantly high precision parts. When compared to grinding process the machining time is comparatively 50% lesser. If the right combination of nose radii, feed rate, cutting speed, depth of cut is used then a better surface finish can be obtained as compare to grinding operations. Here, it is confirmed that these tool offers less machining time, higher surface finish during hard turning but its mechanism is need to be studied.[1]

During hard turning the designing of cutting tool is to be considered and these can be studied by observance of cutting force at various cutting conditions. In the current environment, the performance variables are determined experimentally using a trial and error method. To obtain this design plan, it is necessary to estimate the cutting forces from a basic approach so that the performance of the cutting tools and machine tools can be calculated. An analytical model can also be obtained to the predicted values. In the process of hardened machining such as hard turning

© JournalsPub 2016. All Rights Reserved

and milling, an approach is made for considering the various criteria such as cutting forces, chip formation and surface integrity would be very advantageous for better knowledge of hard machining. This is necessary to understand the study of local mechanism of material removal. Indeed, the mastery of surfaces generated by cutting requires knowledge of cutting mechanisms. When Steel with high mechanical properties is to be turned then special preparations are to be done therefore the purpose of the study is AISI D2 steel. On this steel hard turning test were carried out, with the aim to understand morphology of chip in order to reach the optimize condition. The chips obtained were studied under a scanner electron microscope. Thus various readings proved that the chip morphology is influenced by cutting conditions.[2]

The chips had a white layer, and this layer was observed under scanning electronic microscope (SEM) to study the changes depending on cutting conditions. The study shown, that cutting forces decrease with the increase of cutting speed. However, ANOVA (Analysis of Variance) was used to predict the effect of the cutting conditions on experimental obtained results. Finally, a micro hardness test was carried out to relate the mechanical properties and the microstructures of white layers.

Nakayama (1997) explained the mechanism of saw tooth chip formation, when hardening bearing steel was machined. The saw-tooth chip formation was shown to be produced when shear strain on the surface attain an ultimate value αc over which work material cannot afford**.**

Vyas and Shaw (1999) Saw tooth chip forms when very brittle materials are machined at high speeds and feeds. There are two theories concerning the basic origin of saw tooth chips. The first to appear assumed they are thermal origin while the second assumes they arise due to the periodic developments of cracks in the original surface of the work. Jeffrey (1999) experimentally investigated the effect of tool edge geometry on work material sub-surface deformation and through-thickness residual stresses for machining of AISI 52100 bearing steel with PCBN tool. Gerard Poulachon (2000) The results obtained from quick stop identify the four stages of the formation of a saw tooth chip. From Figure 1, it is studied that a relationship has been established between the chip geometry and the cutting condition. S. Kompella (2001) studied the mechanical properties and characteristics of surface layers in AISI 52100 steel produced when machining with CBN tools.

To analyze the surface layers and mechanical properties, the author used a nano indention (measuring the hardness of white layer) technique, optical microscopy and atomic force microscopy (AFM), John Barry and Gerald Byrne (2002). According to John Barry and Gerald Byrne the formation of saw tooth chips to be a cyclic process. The initial stage in the cycle may be taken as the upsetting of the just beginning segment. [3–5]

EXPERIMENTAL DETAILS

Material

The material studied here is high alloyed steel (type ENX160CrMoV12/AISI D2). The applications of this steel are found in stamping, molding and other drawing process. The as-received structure of the steel, corresponding to a quenched state under nitrogen pressure after being kept for 150 minutes at 1050°C, followed by two tempering to 2 hours at 500°C. The overall hardness of the material is 62 HRC.

Machine

Conventional lathe machine is used for turning process. Here are its specifications:

Sr. No.	Specifications	Range
1.	Spindle speed	32-1200 rpm
2.	Spindle motor power	3 kW
3.	Maximum Turning length	1500mm
4.	Maximum turning diameter	265 mm
5.	Controller	HMT-LTM
6.	Number of station of turret head	8
7.	Weight	1550 kg

Measuring Equipment

(1) Here for microscopic images scanner electron microscope is used.
(2) Lathe tool dynamometer is used for measuring the cutting forces.
(3) Microhardness tester is used for micro hardness test.

Cutting Tool

Hard turning involves special and improved cutting tools for machining which can resist high temperature, hardness and which can also enhance surface quality. Cutting tool insert for hard turning requires special tool holders, improved machinery, and they are also not easily available. Sintered Tungsten carbide cutting tools are very abrasion resistant and can also withstand higher temperatures than standard high speed steel tools. Cemented carbide is a metal matrix composite where tungsten carbide particles are the aggregate and metallic cobalt serves as the matrix. Carbide cutting surfaces are often used for machining through materials such as carbon steel or stainless steel, as well as in situations where other tools would wear away, such as high-quantity production runs. Because carbide tools maintain a sharp cutting edge better than other tools, they generally produce a better finish on parts, and their temperature resistance allows faster machining. Hence in the present work sintered tungsten carbide tool is selected for hard turning. Three cutting tools are selected with three nose radii's i.e. 2mm, 3mm, 5 mm. Table 1 shows the physical properties of cutting tool.

Table 1. *Cutting Tool Physical Properties (Source: Metal Data Handbook, 1990).*

Young's modulus	Bulk modulus	Modulus of rigidity	Hardness(HRC)	Tensile strength	Compressive strength
530–700 GPa	630–650GPa	274 GPa	88	344 MPa	2.7 GPa

Cutting Conditions

The present work is based on observation of machined surface, sub- surface images, chip images, cutting forces at various cutting condition. The complete study consist of observing the micro images of chips, machined surface images on SEM and micro hardness of chips, cutting forces

at various cutting conditions. The experiments are conducted in two parts:

(1) Study of cutting forces: In the first part the objective was to study the effect of cutting parameters on the cutting force. The experiment is performed on the conventional lathe machine with the combination of three cutting parameters as shown in Table 2. Overall 27 experiments were carried out for various combination of cutting factors selected and cutting forces data are collected.

Table 2. *Experimental Levels of Cutting Parameters.*

Feed (mm/rev)	Cutting speed (m/min)	Depth (mm)
0.05	55	0.15
0.1	94	0.25
0.15	157	0.75

(2) Study of chip morphology and machined microstructure: In the second part of experiments the objective was to study the chip morphology, micro hardness variation and micro-structure of machined surface. The parameters selected for chip morphology and micro-hardness test are shown in Tables 3 and Table 4. The parameters selected for machined microstructure are shown in Tables 5–8.

Table 3. *Feed Parameters for the Study of Microimages of Chips and Chip Hardness.*

Nose radius (mm)	Depth (mm)	Speed (m/min)	Feed (mm/rev)
2	1	94	0.05
			0.07
			0.1
			0.15

Table 4. *Speed Parameters for the Study of Microimages of Chips and Chip Hardness.*

Nose radius (mm)	Depth (mm)	Feed (mm/rev)	Speed (m/min)
2	1	0.1	55
			94
			157
			263

Table 5. *Speed Parameters for the Study of Microimages of Machined Surface.*

Nose radius (mm)	Feed (mm/rev)	Depth (mm)	Speed (m/min)
2	0.2	0.5	94
			157
			263

Table 6. *Nose Radius Parameters for the Study of Microimages of Machined Surface.*

Speed (m/min)	Feed (mm/rev)	Depth (mm)	Nose radius (mm)
94	0.2	0.5	2
			3
			5

Table 7. *Depth Parameters for the Study of Microimages of Machined Surface.*

Speed (m/min)	Feed (mm/rev)	Nose radius	Depth (mm)
94	0.2	2	0.5
			1
			1.5

Table 8. *Feed Parameters for the Study of Micro images of Machined Surface.*

Nose radius (mm)	Speed (m/min)	Depth (mm)	Feed (mm/rev)
2	94	0.5	0.05
			0.1
			0.15

RESULTS AND DISCUSSION

In this chapter, a description is presented about the task of data collection and their analysis according to proposed methodology as discussed in Chapter 3. Experimental studies were conducted with different cutting conditions as described in chapter 3 to study influence of cutting forces, chip transition, micro-hardness of chip and micro-structure of machined surface. The results of these experiments are presented in this chapter.

Influence of the Cutting Speed on the Form of Chip

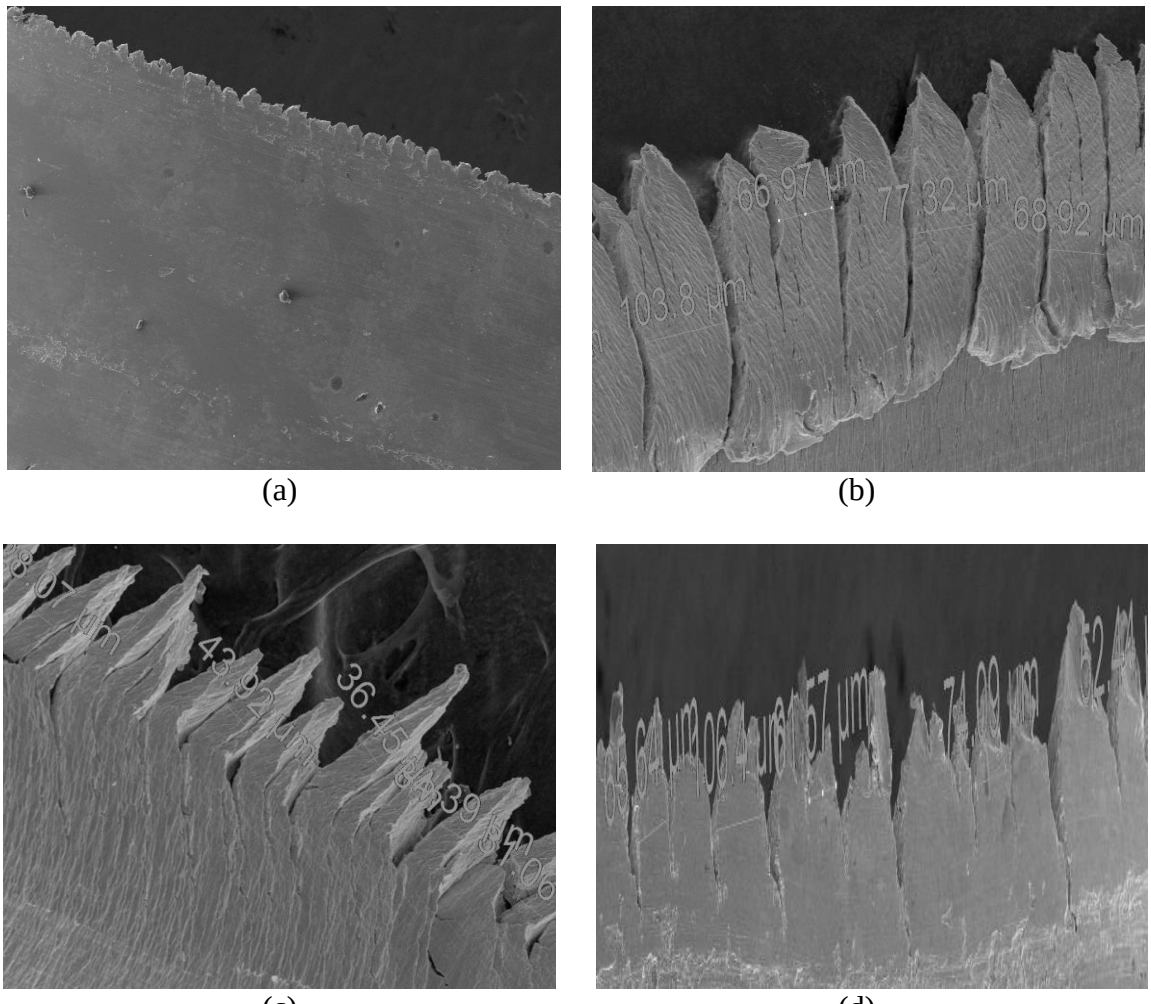
The cutting conditions are f = 0.1 mm/rev, d = 1 mm, cutting speed varies from 55 to 263 m/min. The observed chips are in all

cases of ‘‘saw tooth’’ chip type; they are short and curled at low cutting speed, continuous chips at 55 m/min, elemental between 94 and 263m/min, and reduced to powder at higher speeds. The chip types obtained at different speeds are shown in Table 9 and the micro images of the chips as shown in Figure 1. With the increase in speed the tooth flank starts getting wider.

First the chip tooth forms uniform saw tooth as shown in Figure 1(b) and then the tooth becomes pointed and distorted as shown in Figure 1 and 2. With further increase in speed the cracks occur on the tooth of the chip. With increasing speed the heat generation increases and due to these the temperature increases (Chinchanikar, 2014). [6]

Table 9. *Types of Chip Obtained at Different Cutting Speed.*

Speed (m/min)	Types of chip
55	Continuous Chip
94	Uniform saw tooth chip
157	Non-uniform saw tooth chip
263	Saw-tooth chip with broken tooth



(a) (b)

(c) (d)

Fig. 1. *Chips at Various Cutting Speeds and Constant Feed. 1 mm/rev (a) Continuous Chip (v = 55 m/min), (b) Saw Tooth Uniform Chip (v = 94 m/min), (c) Saw Tooth Nonuniform Chip (v =157 m/min), (d) Saw Tooth Chip With Broken Tooth (v= 263 m/min).*

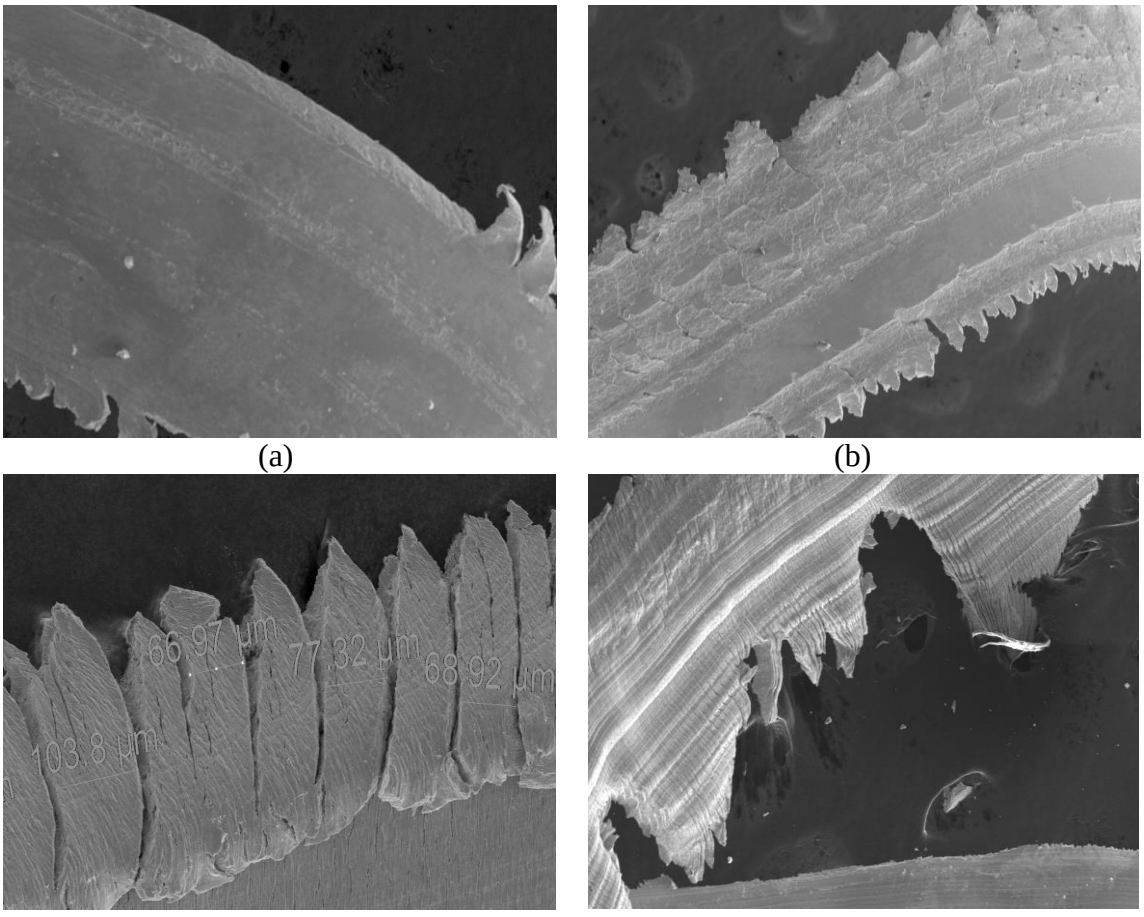
Influence of the Feed on the Form of Chip

The cutting conditions are V = 94 m/min, d =1 mm, feed rate varies from 0.05 to 0.15 mm/ rev. The chips are continuous chips at f =0.05 mm/rev and above this rate, they become discontinuous, and at very high feed rates they are reduced to powder. The chip types obtained at different feeds are shown in Table 10 and the micro images of the chips as shown in Figure 2.

At 0.05 mm/rev the chip has a continuous shape and as the feed is increased to 0.07 mm/rev the chip is slightly continuous and slightly saw-tooth and it means the chips are not completely saw-tooth and it can be named as wavy chips. At 0.1 mm/rev the chip takes the complete shape of saw-tooth and tooth flanks are also uniform. With further increase in feed the chip formation remains saw-tooth but the tooth flanks becomes wider and non-uniform.

Table 10. *Types of Chip Obtained at Constant Speed.*

Feed (mm/rev)	Types of chip
0.05	Continuous chip
0.07	Wavy chips
0.1	Uniform Saw tooth chips
0.15	Non- uniform saw tooth chip



(a) (b) (c) (d)

Fig. 2. *Chips at various feeds and constant speed 94 m/min (a) Continuous chips (feed = 0.05 mm/rev) (b) Wavy Chips (feed = 0.07 mm/rev) (c) Uniform saw tooth chip (feed = 0.1 mm/rev) (d) Non uniform saw tooth chip (feed = 0.15 mm/rev).*

Although the saw-tooth chip is formed with both increasing speed and increasing feed but increase in speed generates saw tooth more quickly than increasing feed and the increasing speed involves non-uniform and distorted tooth flanks and increasing feed involves uniform and less distorted tooth flanks.

Chip Hardness

Chip hardness was also measured at various cutting speed with constant feed, depth and nose radius as shown in Table 11. Figure 3 shows the chip hardness increases with increase in speed and this is probably due to increase in temperature with cutting speed due to increased heat generation. (chinchanikar, 2014).

Table 11. *Chip Micro-hardness at Increasing Speed with Constant Depth Feed and Nose Radius.*

Nose radius (mm)	Depth (mm)	Feed (mm/rev)	Speed (m/min)	Chip micro-hardness (HV)
2	1	0.1	55	403
			94	407
			157	374
			263	430

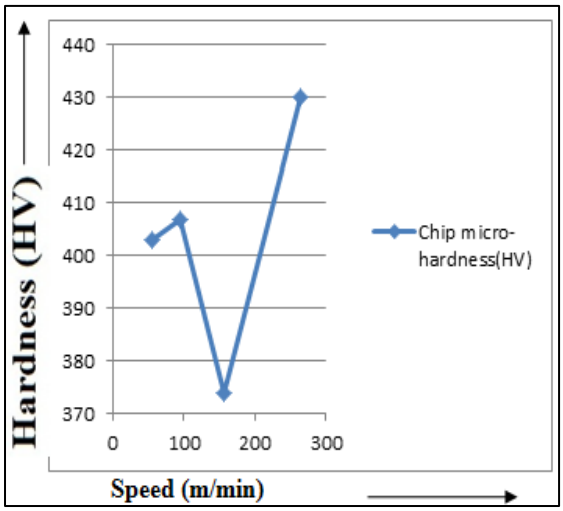


Fig. 3. *Variation of Chip Hardness (HV) With Speed at Constant Feed, Depth and Nose Radius.*

Chip hardness was measured at various feed with constant depth, speed and nose radius as shown in Table 12. Figure 4 shows the chip hardness increases with increases in feed (Table 13).

Chip hardness was measured at various depth with constant speed, feed and nose radius. Figure 5 shows the chip hardness is almost constant with increasing in depth.

Table 12. *Chip Micro-hardness at Increasing Feed with Constant Speed, Depth and Nose Radius.*

Nose radius (mm)	Depth (mm)	Feed (mm)	Speed (m/min)	Chip micro-hardness (HV)
2	1	94	0.05	404
			0.07	405
			0.1	407
			0.15	431.8

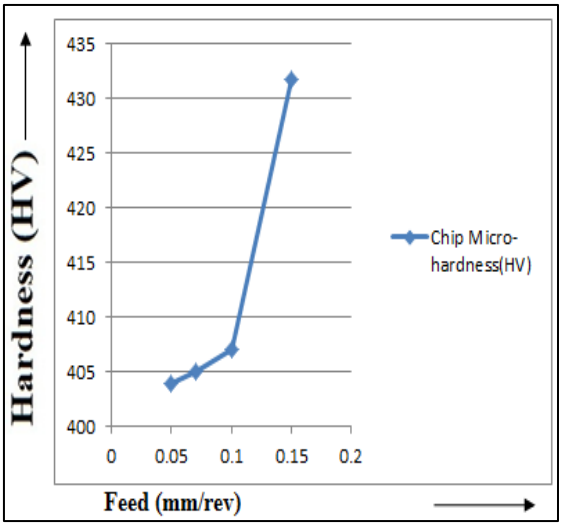


Fig. 4. *Variation of Chip Hardness (HV) With Feed at Constant Speed, Depth and Nose Radius.*

Table 13. *Chip Micro-hardness at Increasing Depth with Constant Feed, Speed and Nose Radius.*

Nose radius (mm)	Feed (mm/rev)	Speed (m/min)	Depth (mm)	Chip micro-hardness (HV)
2	1	94	0.5	428.3
			1	431.8
			1.5	430.2
			2	429.2

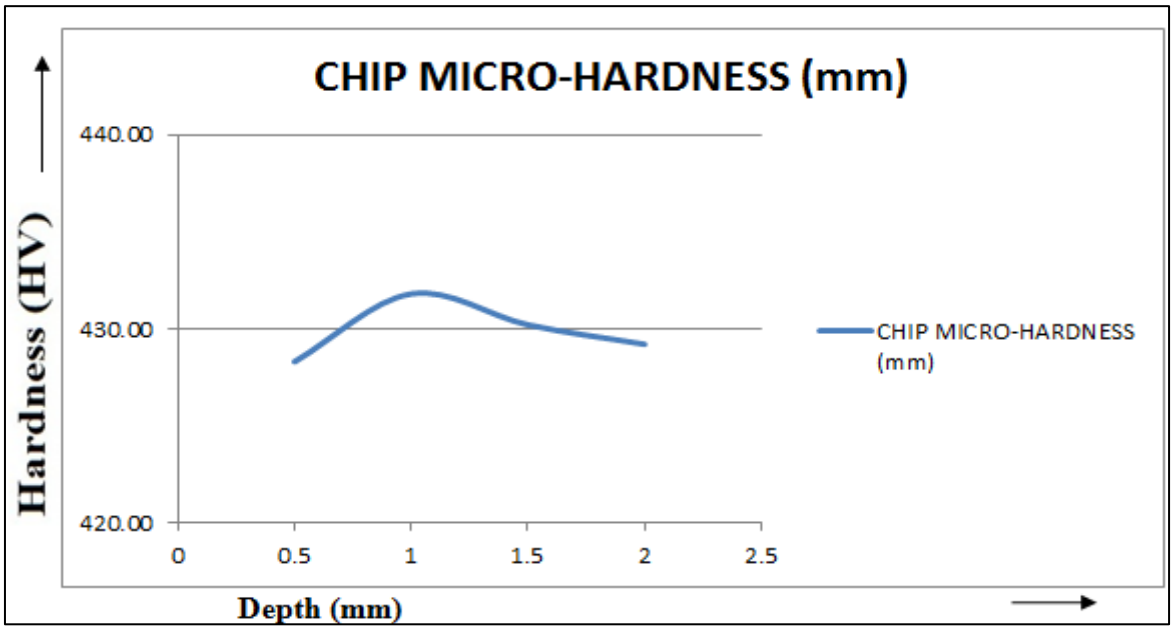


Fig. 5. *Variation of Chip Hardness (HV) With Depth at Constant Speed, Feed and Nose Radius.*

With the increase in speed the chip hardness first increases then decreases and then again increases as shown in Figure 3 and this is due to increase in temperature which may impart some ductility and the chip has very less chances of detachment as compared to that in case of increased feed and depth of cut.

With the increase in feed the chip hardness continuously increases without any decrease as shown in Figure 3 and with increasing feed the temperature does not increase that much as comparison to speed. Therefore chip has more chances of detachment as comparison to speed.

With the increase in depth the chip hardness is almost remains constant as shown in Figure 5 and as comparison to speed and feed the chip hardness is initially more to speed and depth. The depth involves more removal of material and consequently hardness also increases therefore chip has more chances of detachment as comparison to speed and depth.[7]

Surface and Subsurface Deformation and White Layer Formation

Experiments were conducted to study the surface micro-structure with a view to examine the SEM images surface and sub-surface cracks and white layer formation. The experiments were done at done at different combination of parameters. The results are discussed as follows:

(a) Case 1 – Increasing Nose Radius

The experiments were done at a feed = 0.2 mm, speed = 94 m/min, depth = 0.5 mm and with increasing nose radius from 2, 3 and 5 mm**.**

(1) Nose radius = 2 mm, feed= 0.2 mm/rev, speed= 94 m/ min, depth = 0.5 m

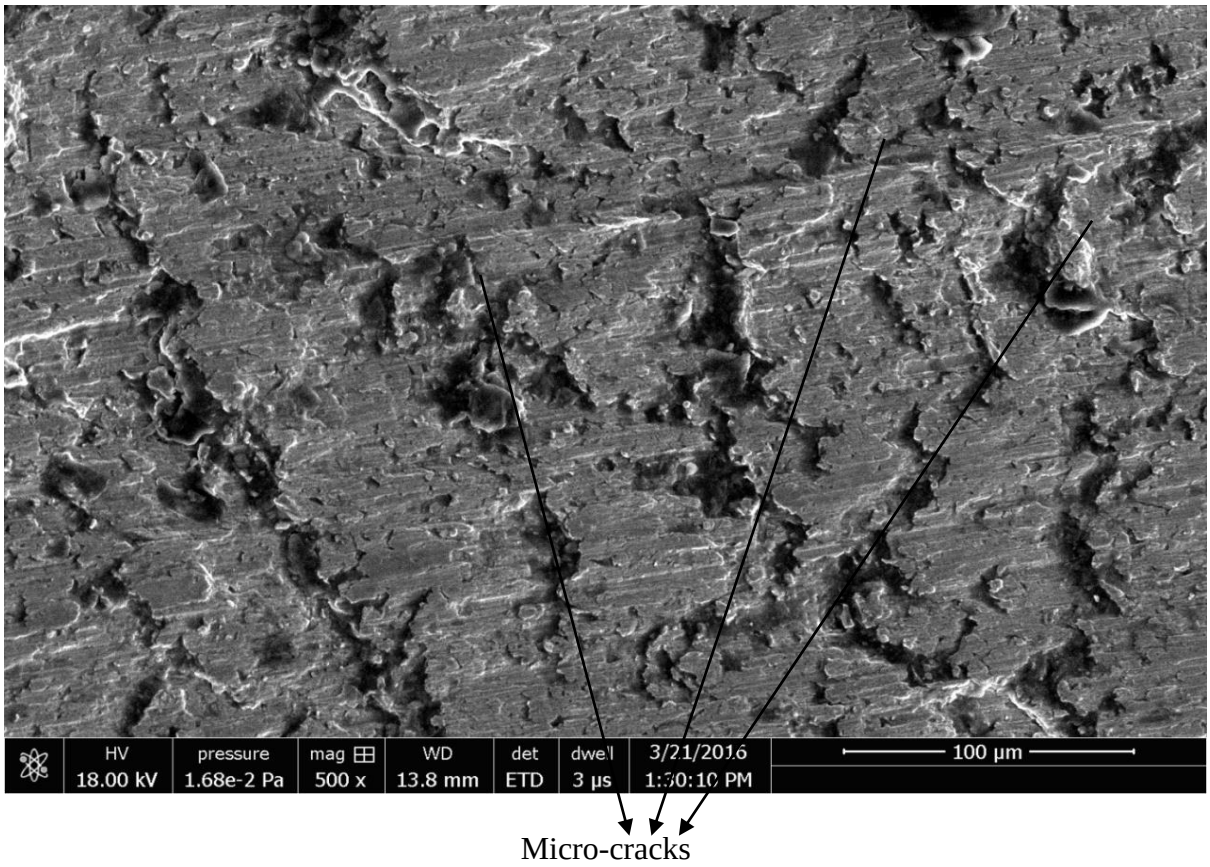


Fig. 6. *Micro images of machined surface at Nose radius= 2mm, speed=94m/min, feed, =.2mm, Depth = 0.5 mm.*

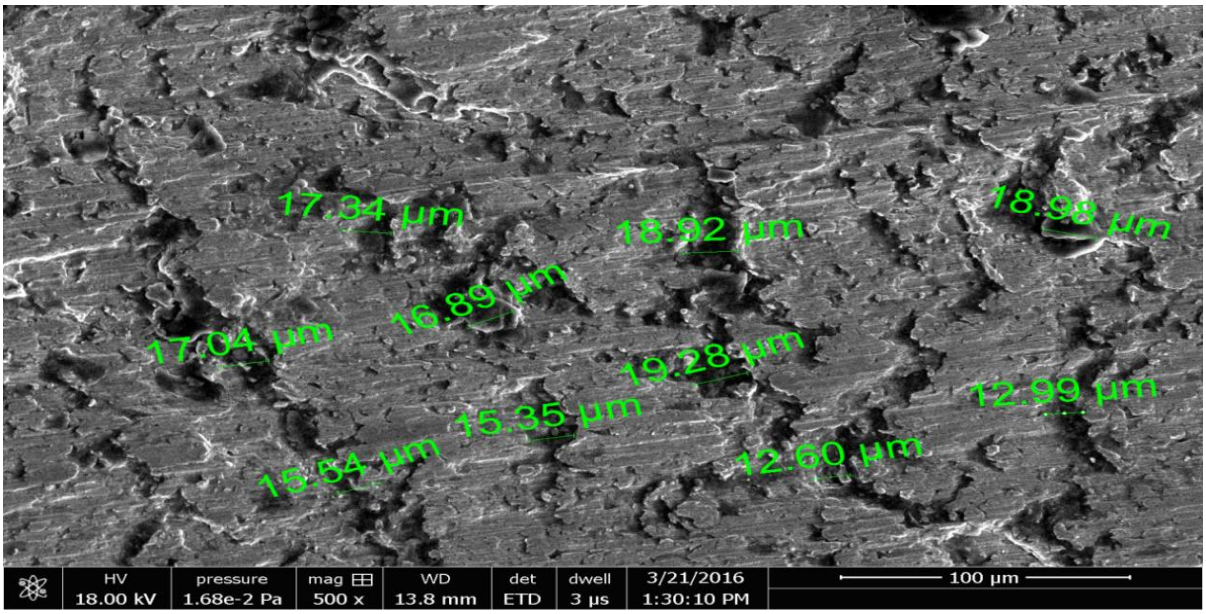


Fig. 7. *Shows the Length of Various Cracks at Nose Radius= 2 mm, Speed=94 m/min, Feed, =0.2mm, Depth = 0.5 mm.*

(2) Nose radius =3 mm, feed= 0.2mm/rev, speed= 94 m/min, depth = 0.5mm

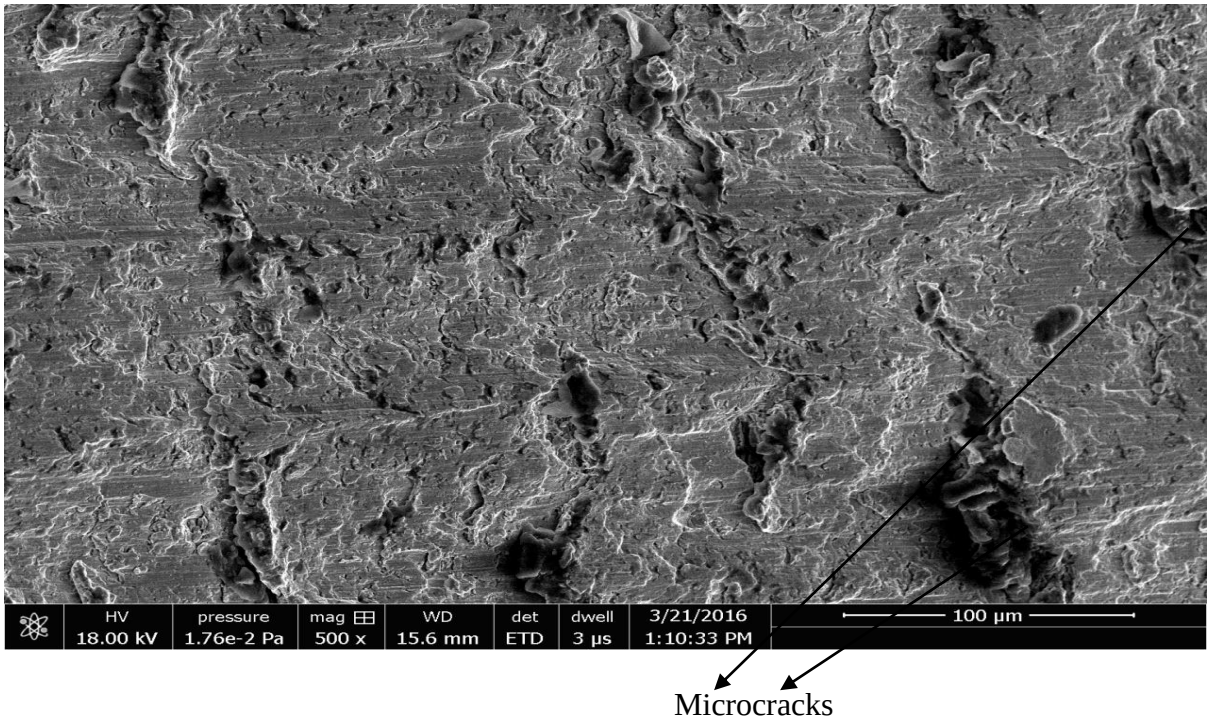


Fig. 8. *Microimages of Machined Surface at Nose Radius= 3 mm, Speed=94 m/min, Feed, =0.2 mm, Depth = 0.5 mm.*

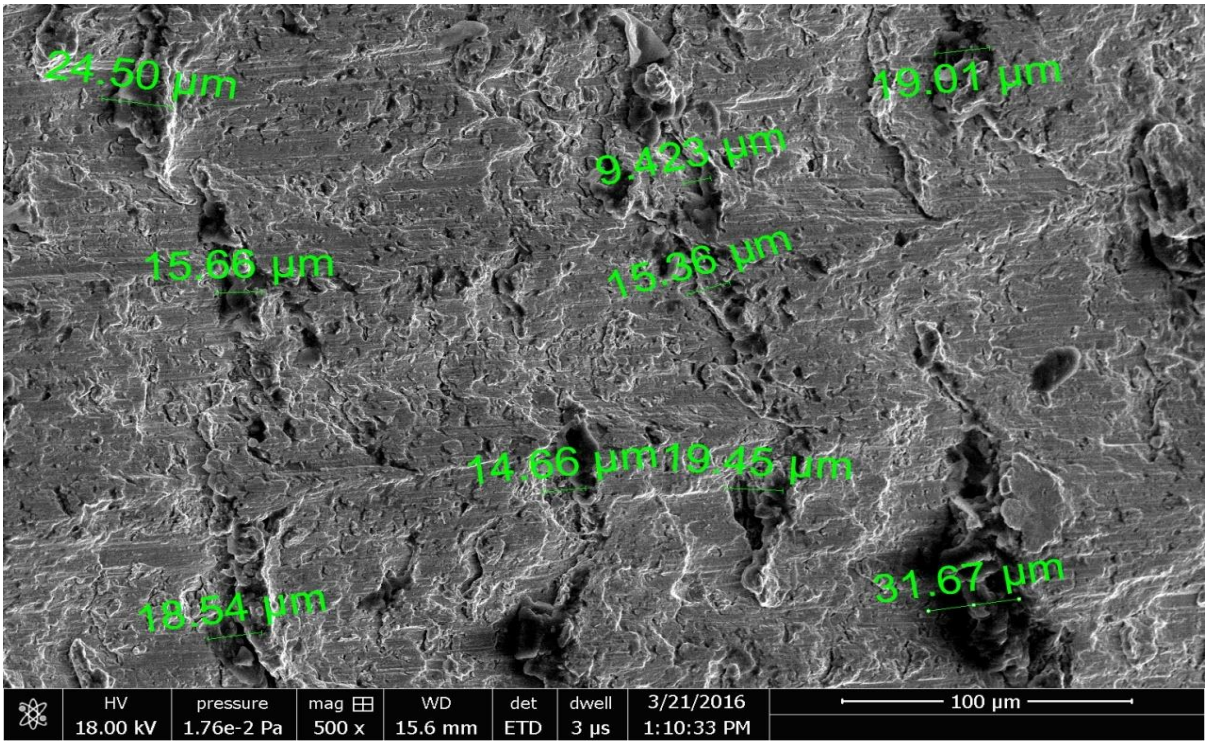


Fig. 9. *Shows the Length of Various Cracks at Nose Radius= 3 mm, Speed=94 m/min, Feed, =0.2mm, Depth = 0.5 mm.*

(3) Nose Radius = 5 mm, feed = 0.2mm/rev, speed = 94 m/min, depth = 0.5 mm

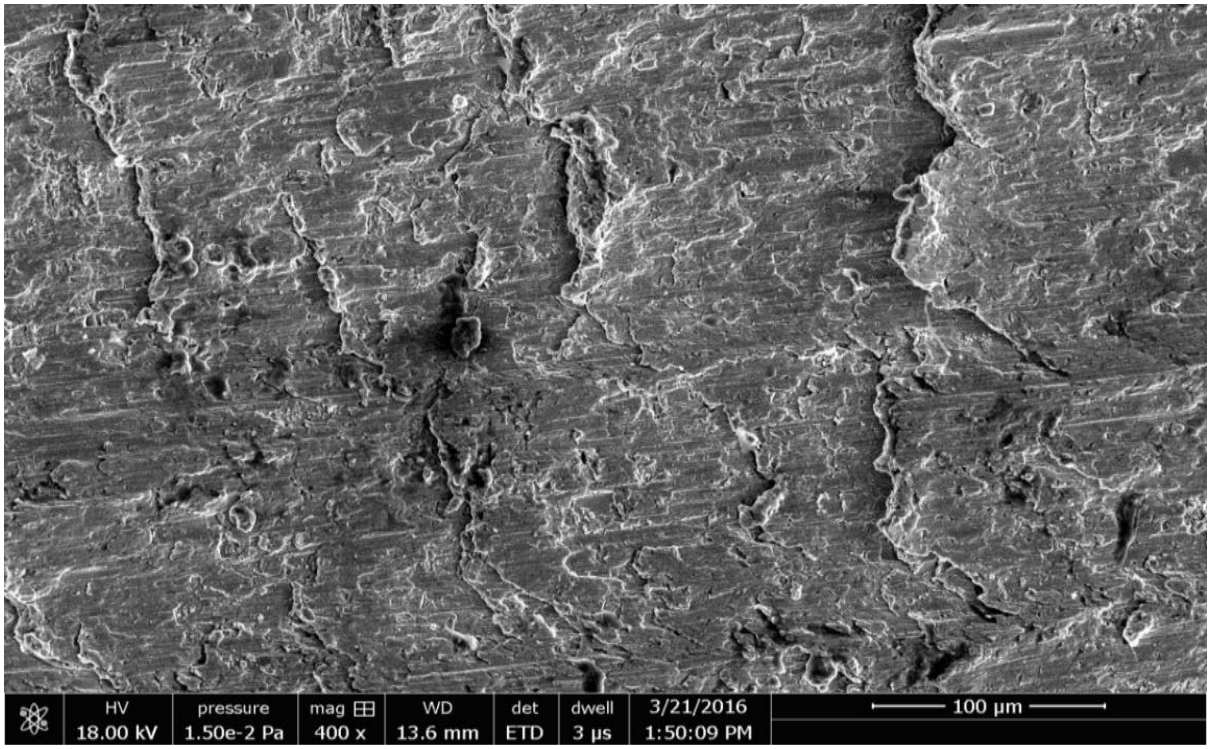


Fig. 10. *Microimages of Machined Surface at Nose Radius= 5 mm, Speed=94 m/min, Feed, =0.2 mm, Depth = 0.5 mm.*

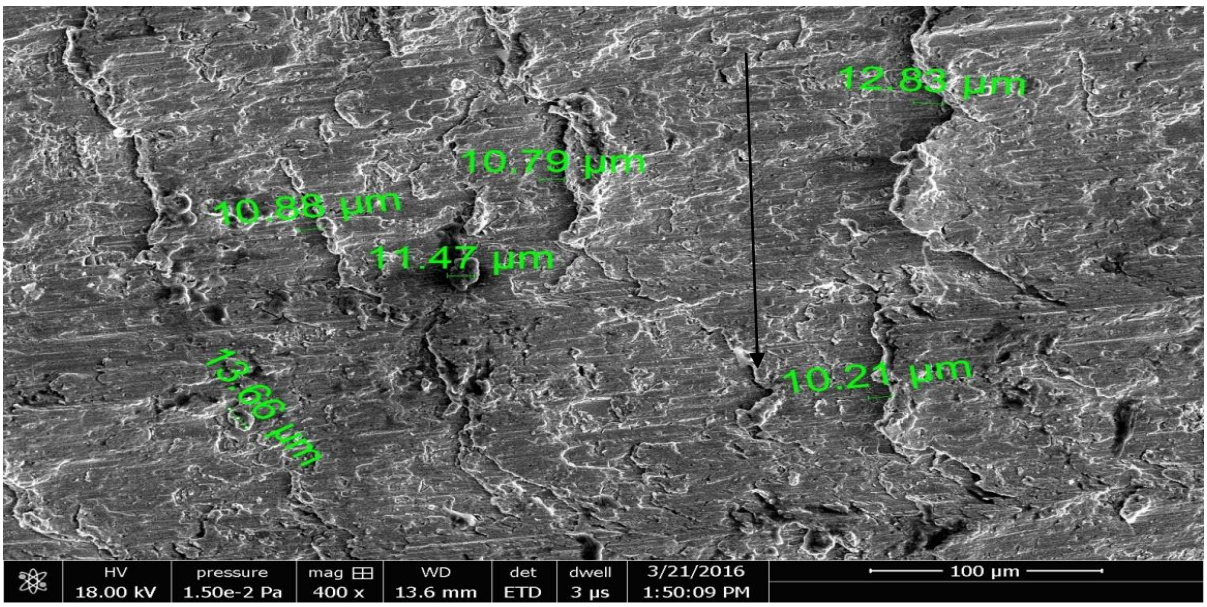


Fig. 11. *Shows the Length of Various Cracks at Nose Radius= 5 mm, Speed=94 m/min, Feed, =0.2mm, Depth = 0.5 mm.*

As shown in Figures 6–11 the micro-cracks and cavities becomes less and white layer formation thickness also reduces with increasing nose radius. Therefore tool with large nose radius can be favorable for cutting conditions. The lengths of the cracks are varying from minimum of 10.24 µm to 13.66 µm which is much less than with the nose radius of 2 mm, 3 mm respectively.

Micro cracks, cavity, and white layer formation relates to the fatigue life and surface quality of machine components. Here the tool has a nose radius of 5 mm which provides round cutting edge which leads to decrease in the density of cracks and cavities as shown in Figure10. White layer thickness also reduces to 1.75 µm and hence fatigue life and surface quality of machined work piece improves with increase in nose radius. [8]

Case 2- Increasing Speed

(4) Nose radius = 2 mm, feed = 0.2 mm, speed = 157 m/min, depth = 0.5 mm

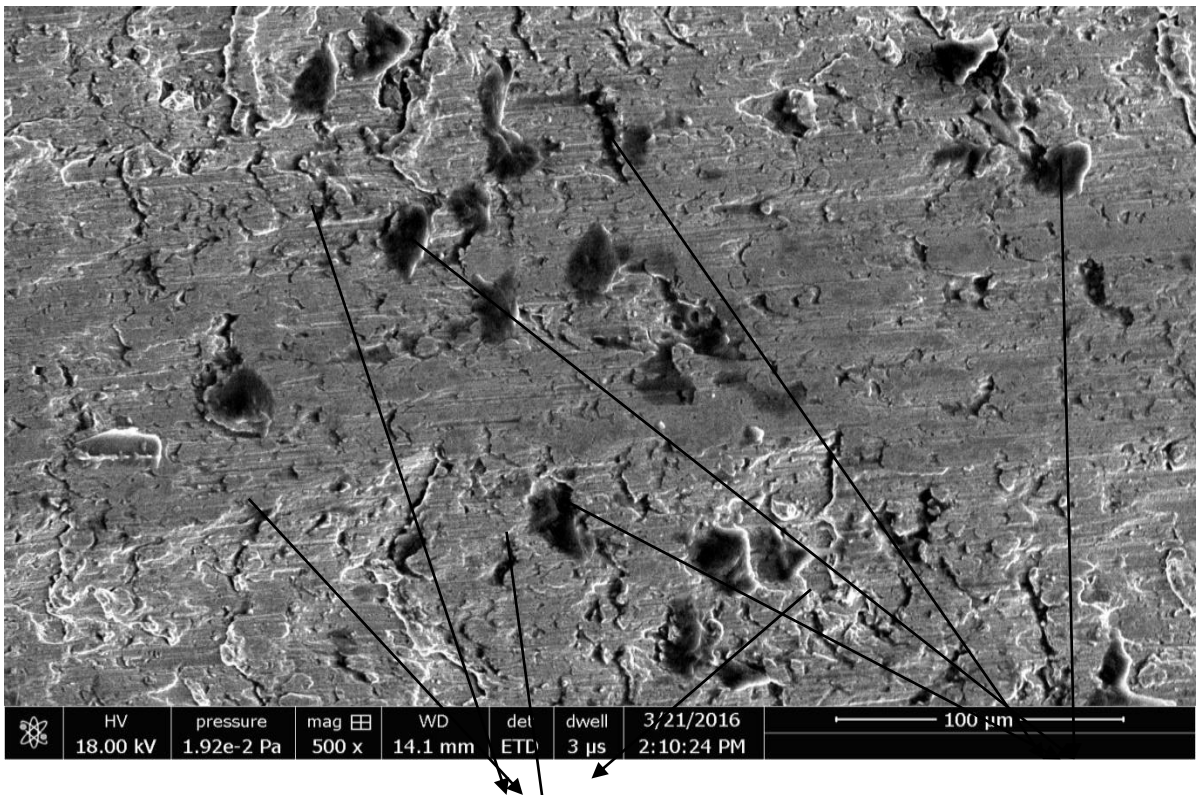


Fig. 12. *Micro Images of Machined Surface at Nose Radius = 2 mm, Feed = 0.2 mm, Speed = 157 m/min, depth = 0.5 mm.*

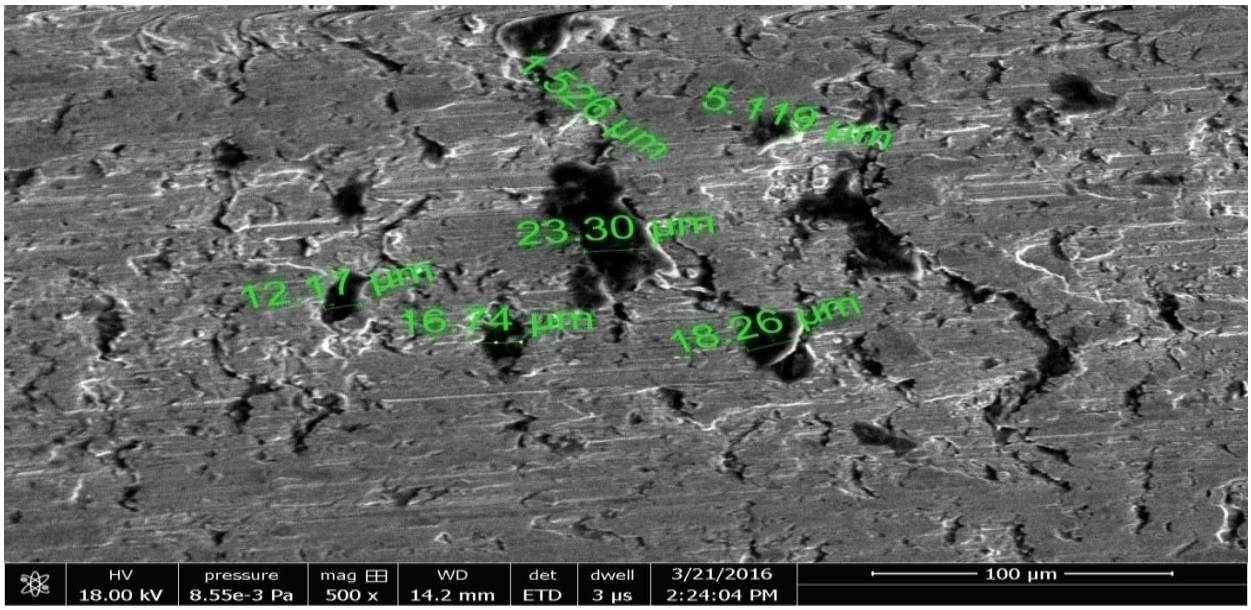
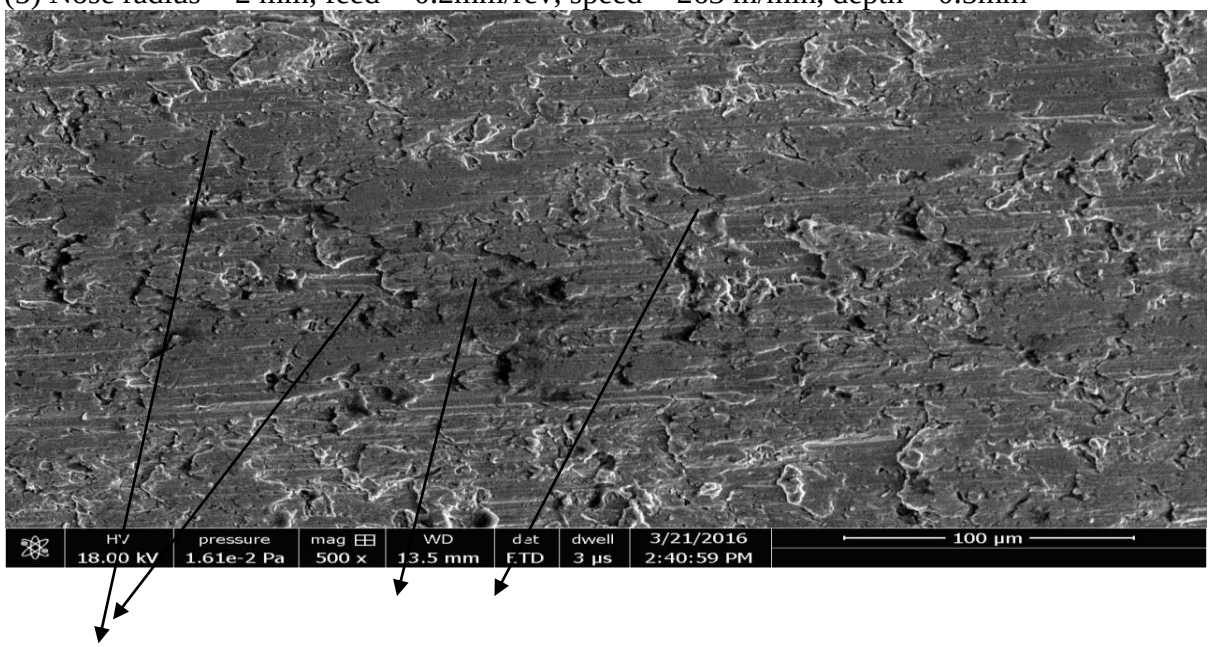


Fig. 13. *Shows the Length of Various Cracks at Nose Radius = 2 mm, feed = 0.2mm, Speed = 157 m/min, Depth = 0.5 mm.*

(5) Nose radius = 2 mm, feed = 0.2mm/rev, speed = 263 m/min, depth = 0.5mm



Chip particles Micro- cracks and Cavities

Fig. 14. *Microimages of Machined Surface at Nose Radius = 2 mm, Feed = 0.2mm/rev, Speed = 263 m/min, Depth =0.5 mm.*

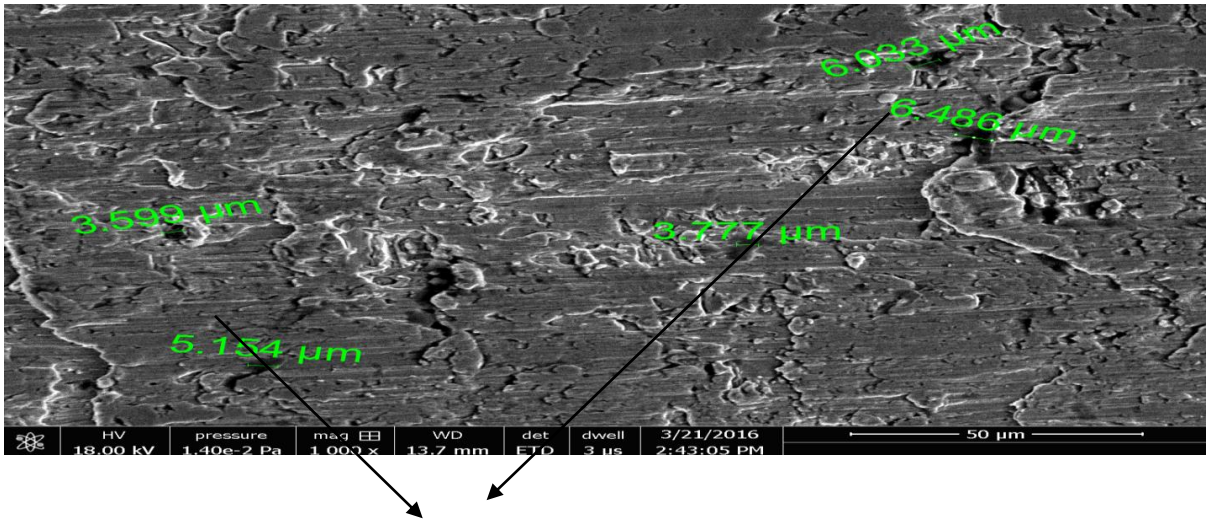


Fig. 15. *Shows the Length of Various Cracks and White Layer Thickness at Nose Radius = 2 mm, Feed = 0.2mm, Speed = 263 m/min, Depth = 0.5 mm.*

The white layer formation thickness increases as shown in Figure 15 and that is about 3.5µm and 3.7 µm. Although micro cracks occur at low as well as high cutting speed but the density of these micro cracks is less at a higher cutting speed. It is believed that the lower density of surface micro cracks at a higher cutting speed is attributed to increase in cutting temperature which leads to thermal softening and local ductility of carbide particles in the vicinity of the machined surface.

Figure 12 reveal the sub-surface structure where large carbide is forced to deform in the vicinity of the surface due to local ductility caused by cutting temperature and pressure. However, lower deformability of carbide particle cause micro cracks beneath the machined surface where the effect of cutting temperature diminishes.

Case 3: Increasing Depth

(6) Nose radius = 2 mm, feed = 0.2 mm/rev, speed= 94 m/min, depth = 1 mm

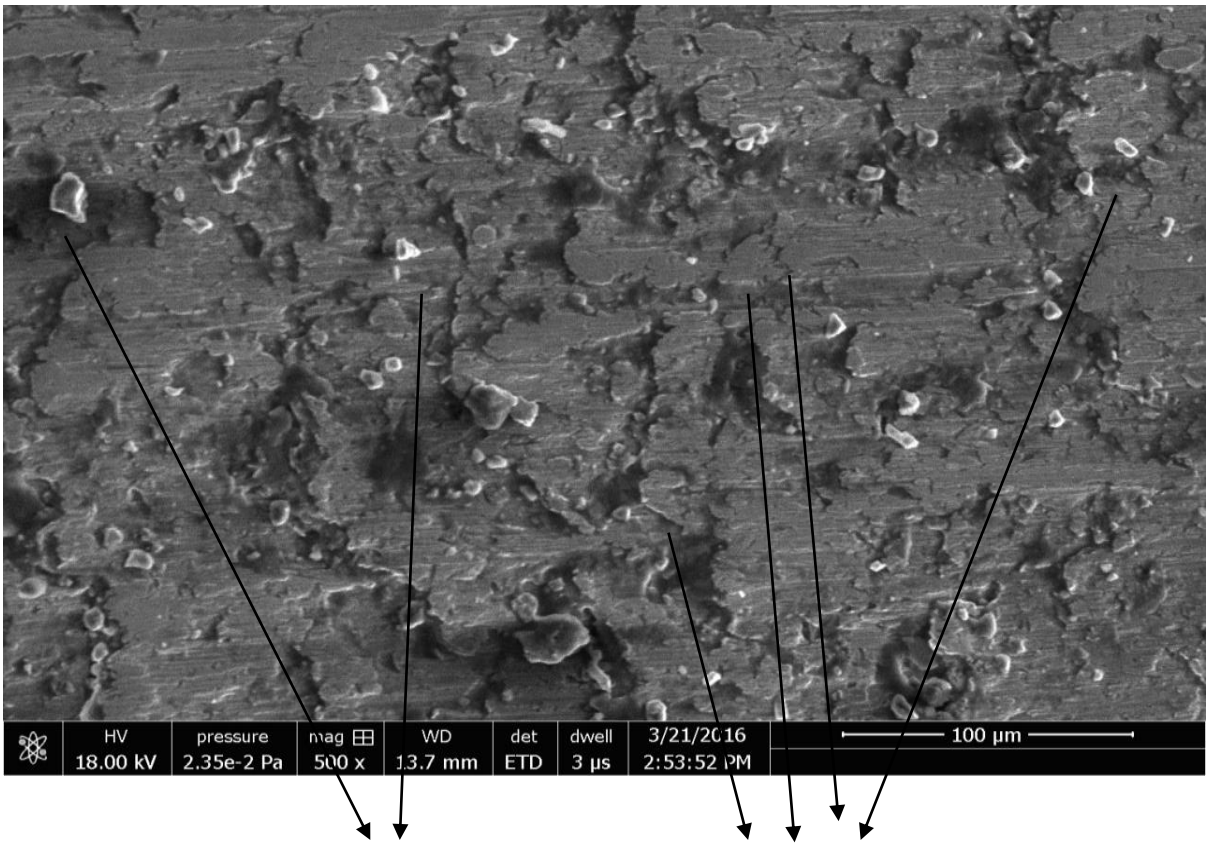


Fig. 16. *Microimages of Machined Surface at Nose Radius = 5 mm, Feed = 0.2 mm/rev, Speed= 94 m/min, Depth = 1 mm.*

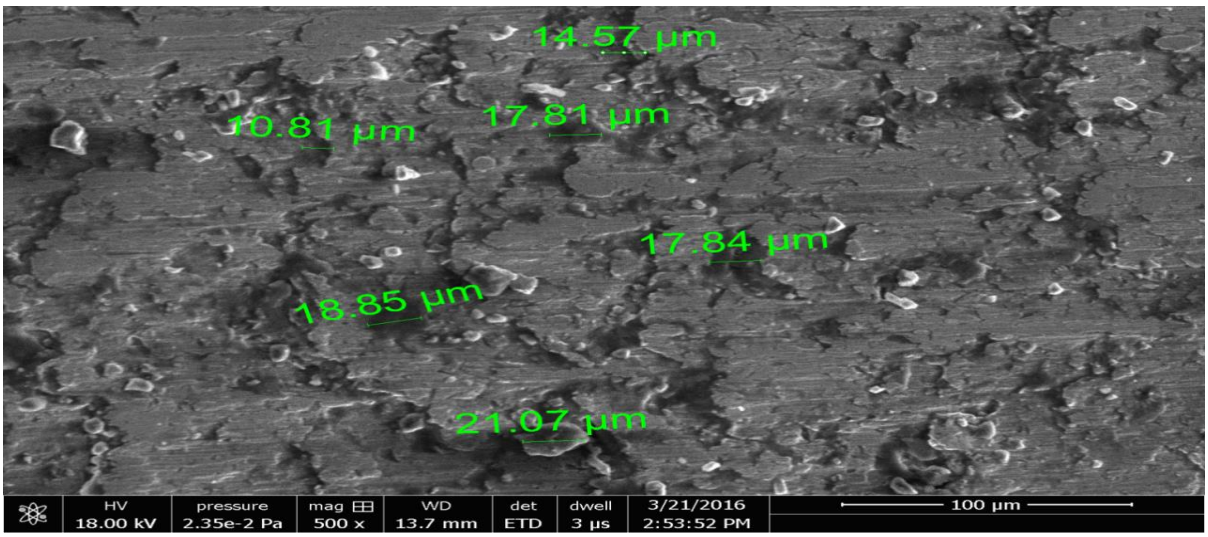


Fig. 17. *Shows the Length of Various Cracks at Nose Radius = 2 mm, Feed = 0.2 mm/rev, Speed= 94 m/min, Depth = 1 mm.*

(7) Nose radius = 2 mm, feed = 0.2 mm, speed = 94 m/min, depth = 1.5 mm

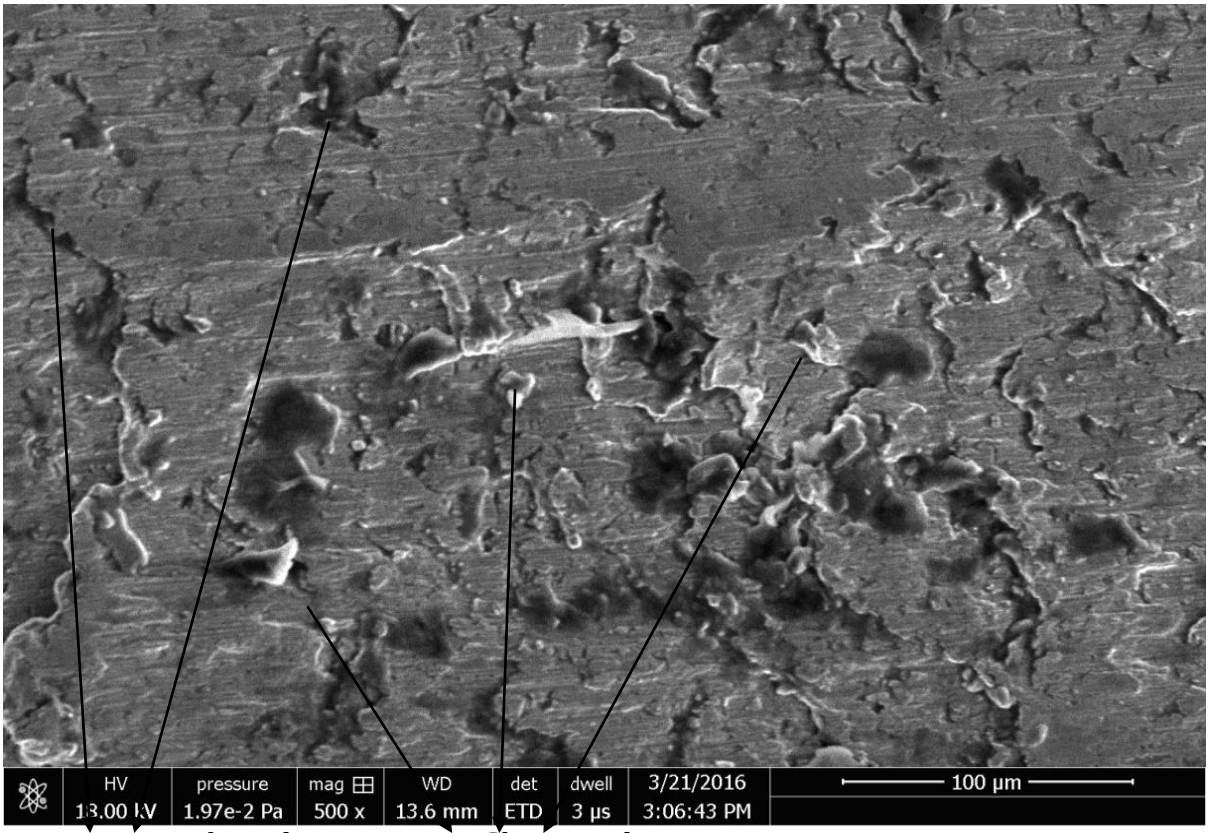


Fig. 18. *Microimages of machined Surface at Nose Radius = 2 mm, Feed = 0.2 mm/rev, Speed= 94 m/min, Depth = 1.5 mm.*

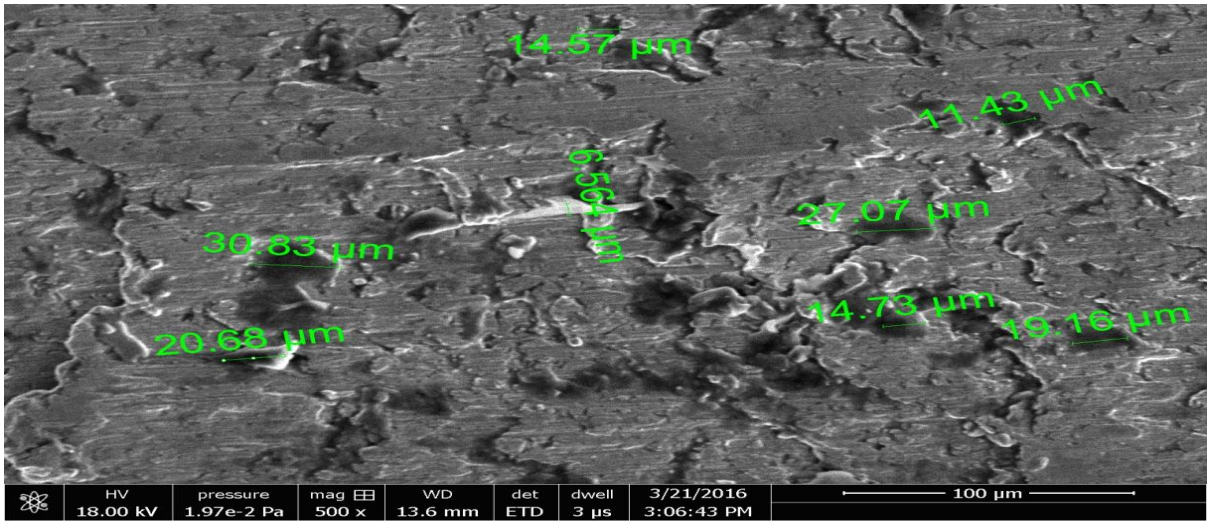


Fig. 19. *Shows the Length of Various Cracks at Nose Radius = 2 mm, Feed = 0.2mm/rev, Speed= 94 m/min, Depth = 1.5 mm.*

Figures 16–19 reveal that with further increase in depth the white layer formation thickness decreases i.e. the white layer thickness is about 269.8 nm and 1.4 µm which are way lesser than comparison to increase in speed but the density of chip particles increases with increase in depth.

Case 3: Increasing feed

(7) Nose radius =2 mm, feed = 0.4mm/min, speed = 94 m/min, Depth = 1 mm

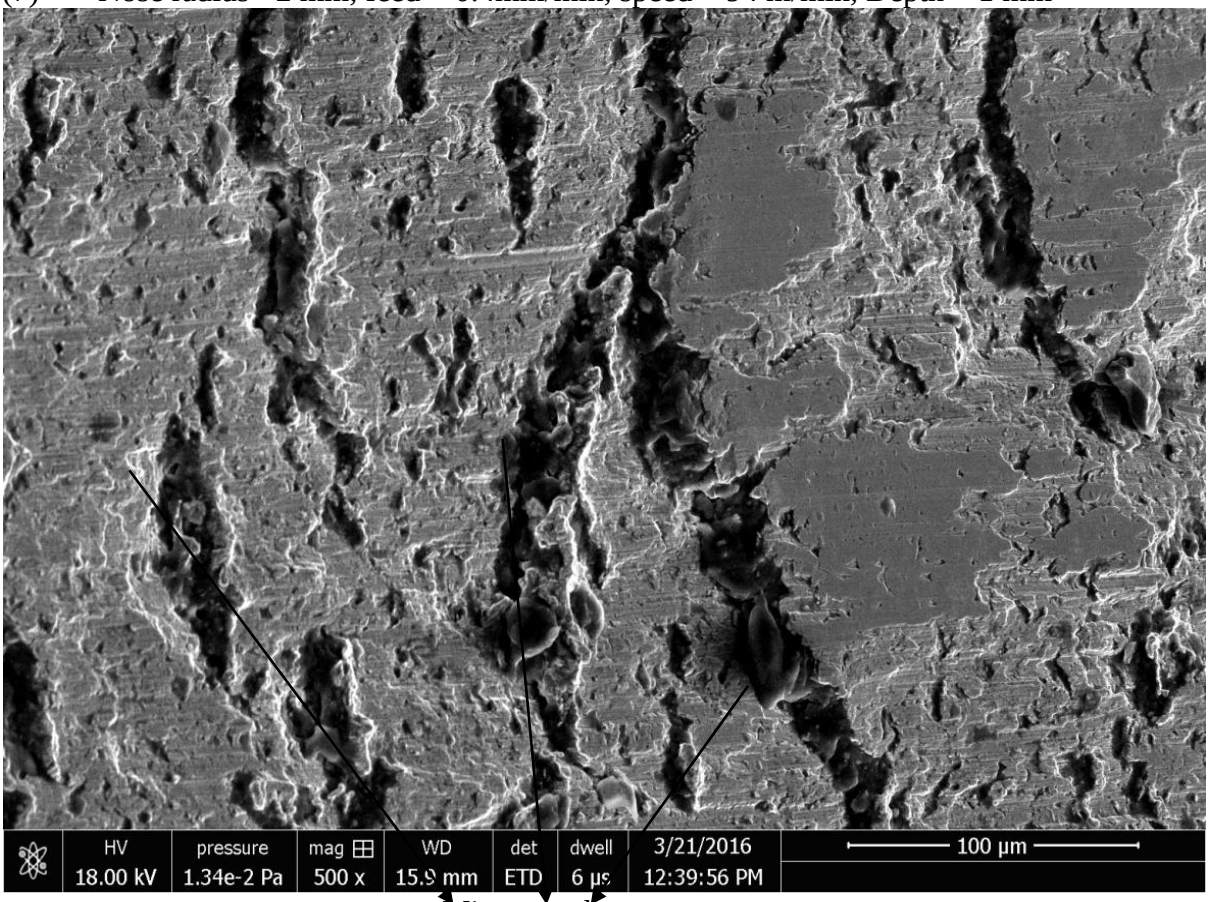


Fig. 20. *Microimages of Machined Surface at Nose Radius = 2 mm, Feed = 0.4mm/rev, Speed= 94 m/min, Depth = 1 mm.*

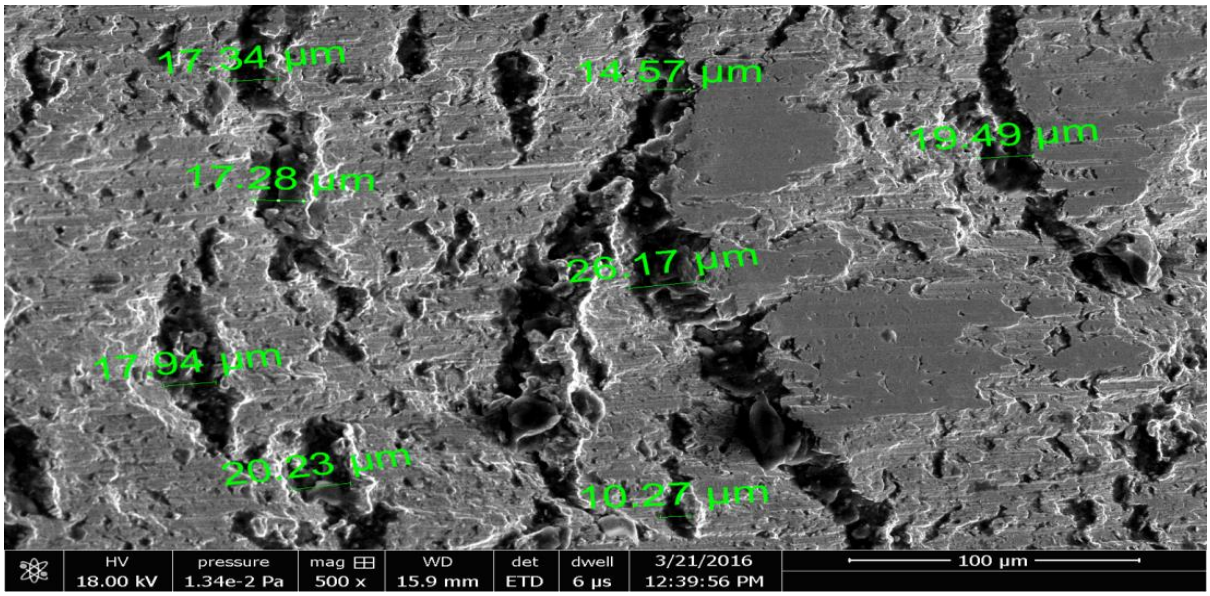


Fig. 21. *Shows the Length of Various Cracks at Nose Radius = 2 mm, Feed = 0.4 mm/rev, Speed= 94 m/min, Depth = 1 mm.*

(9) Nose radius = 2 mm, feed = 0.75 mm/rev, speed = 94 m/min, Depth = 1 mm

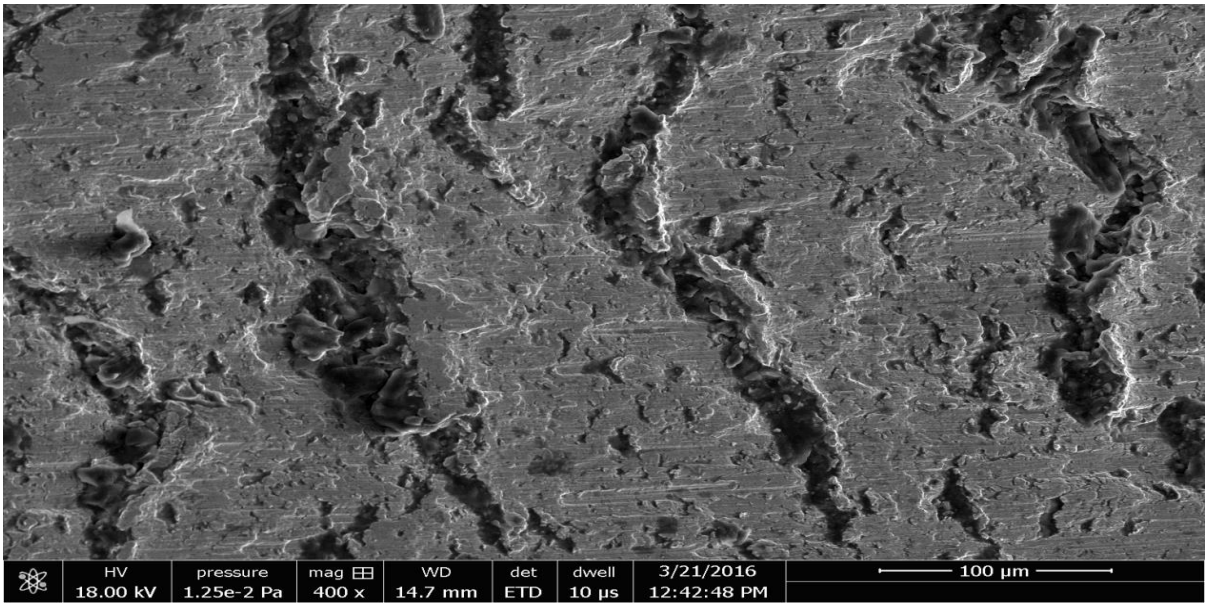


Fig. 22. *Microimages of Machined Surface at Nose Radius =2 mm, Feed = 0.4 mm/min, Speed = 94 m/min, Depth = 1mm.*

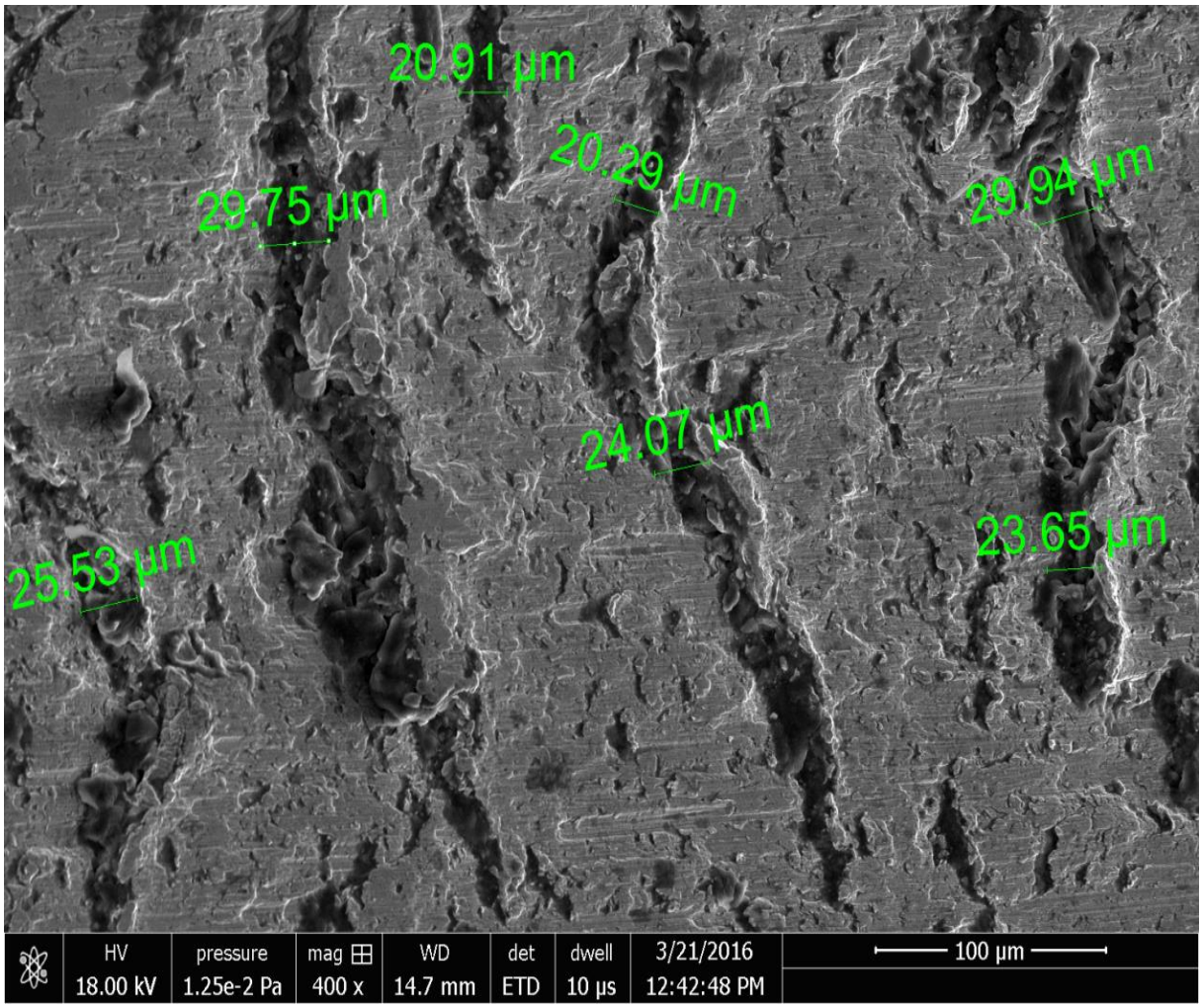


Fig. 23. *Shows the Length of Various Cracks Nose Radius = 2 mm, Feed = 0.75 mm/rev, Speed = 94 m/min, Depth = 1 mm.*

Figures 19–22 reveal that with increase in feed the cracks become long and wide i.e. it varies from minimum of 20 µm to maximum of 32µm which is higher than other cutting conditions. White layer formation thickness is lesser than depth, speed and nose radius and the adhered chip particles density is almost negligible. The main source of surface micro cracks is work piece material non homogeneity caused by local differences in the material element concentration and as well as the existence of chromium carbide particles. Although micro cracks occurs in all the cutting conditions but density of these micro-cracks is less with increasing speed as comparison to increase in feed and depth. To a greater extent, these damages influence the performance of product. Micro-cracks existing on the surface produced reduced the fatigue resistance of the product. White layer formation and thickness decreases with increase in nose radius and increases with increase in cutting speed, while it is less with increase in feed and depth of cut. White layer thickness which is supposed to be a result of temperature created on the surface of work piece and with increase in speed the temperature becomes highest. From all these discussions this is concluded that increasing speed can cause poor surface quality and reduces fatigue life and this is followed by depth and then feed.[9]

Analyses of Cutting Forces

The feed cutting force F_a is relatively weak with regard to the tangential-cutting force F_t. A statistical study was carried out in the present work using "ANOVA" to establish

the effect of cutting parameters employed in the study are given in Table 14. The cutting forces related to the mechanical properties of work material and they influence the process of chip formation. The cutting forces obtained at these parameters are presented to variance analysis using MINITAB 1. The results are shown in Table 15.

Table 14. *Experimental Levels for Cutting Parameter.*

Feed (mm/rev)	Speed (m/min)	Depth (mm)	Cutting force (kg F)
0.05	55	0.15	20
		0.25	10
		0.75	20
	94	0.15	48
		0.25	15
		0.75	20
	157	0.15	26
		0.25	51
		0.75	56
0.1	55	0.15	34
		0.25	12
		0.75	23
	94	0.15	45
		0.25	12
		0.75	17
	157	0.15	48
		0.25	56
		0.75	58
0.15	55	0.15	54
		0.25	15
		0.75	25
	94	0.15	52
		0.25	22
		0.75	30
	157	0.15	44
		0.25	63
		0.75	64

Table 15. *Analysis of Variance*.

Source	DF	ADJ SS	ADJ MS	F-Value	P-value
Feed	2	601	330.48	8.90	0.009
Speed	2	4012.5	2006.26	59.43	0.000
Depth	2	73407	367.37	10.88	0.005
Feed * Speed	4	144.6	36.15	1.07	0.431
Feed * Depth	4	145.7	36.43	1.08	0.428
Speed * Depth	4	2553.5	638.37	18.91	0.000
Error	8	270.1	33.76		
Total	26	8462.1			

For the cutting force the cutting speed is the most significant parameter followed by depth and then feed. Also, the Interaction term of speed and depth of cut of the model showed significance effect followed by interaction of feed, depth and feed, speed.

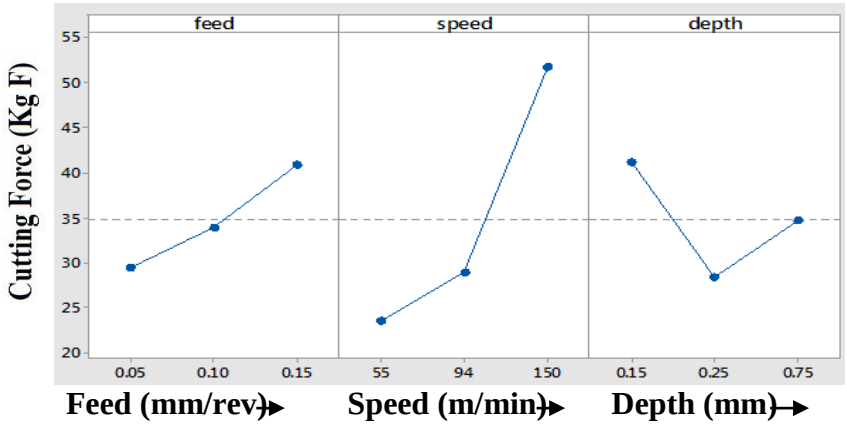


Fig. 24. *Variation of Cutting Force With Respect to Feed, Speed and Depth.*

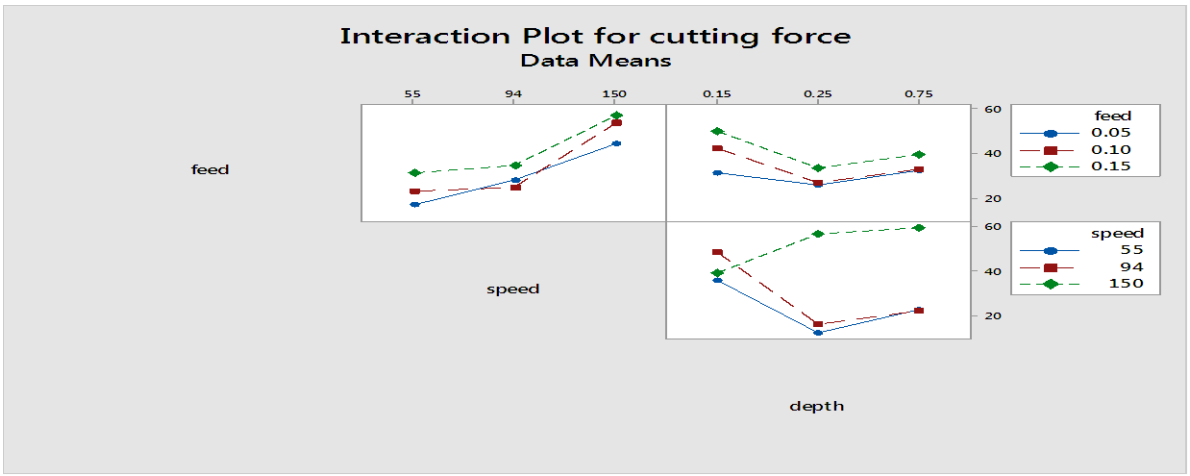


Fig. 25. *Interaction between Speed, Depth, Feed and Their Variation with Cutting Force. (kg F).*

As from the Figures 24 and 25 it is clear that the cutting force increases with increase in speed and feed and in case of depth it decreases then increases. As observed from the graphs the cutting speed highest influence on cutting force. The interaction plot suggests that the interaction of speed and depth has highest influence on cutting force.

The cutting force increases with increase in feed and increases in speed and it slightly decreases with increases in depth but again increases. As predicted by ANOVA the speed has highest influence over it and it also indicates that cutting force is also related with chip morphology and micro –structure of machined surfaces.[10]

CONCLUSIONS

The main conclusions from the present work are as follows.

(1) By ANOVA method this is predicted that cutting speed has highest significant on cutting force followed by depth and feed. Interaction of speed and depth has highest significant effect on cutting force followed by speed and feed, feed and depth.

(2) Saw tooth are formed with increasing feed, speed, and depth of cut.

(3) With increasing speed the chip tooth flank becomes distorted and non-uniform and increasing feed also produces saw-tooth chip but the chip has uniform tooth flank and less distorted.

(4) Chip micro hardness increases with increase in speed and feed but it almost remain constant with increasing depth.
(5) Cutting tool with increasing nose radius produces less micro-cracks and white layer formation with less thickness on machined surface.
(6) Increasing speed involves carbide decomposition and white layer formation with larger thickness on machined surface which results because of change in the phase of machined surface and increasing depth involves detachment of chip particles and it affects the machined surface and increasing feed produces wider cracks. Hence increasing speed has highest effect on surface quality of machined surface followed by increasing speed, depth, feed and nose radius.

REFERERENCES

1. Molinari A., Musquar C., Sutter G. Adiabatic shear banding in high speed machining of Ti-6Al-4V: experiments and modelling, *Int J Plast*. 2002; 18: 443–59p.
2. Sutter G. Chip geometries during high speed machining for orthogonal cutting conditions, *Int J Mach Tools Manuf*. 2005; 45: 719–726p.
3. Horting C., Svendsen B. Simulation of chip formation during high speed cutting, *J Mater Process Technol.* 2007; 186: 66–7p.
4. Komanduri R., Brown R.H. The mechanics of chip segmentation in machining, *J Eng Ind*. 1981; 103: 33–51p.
5. Konig W. Machining hard materials with geometrically defined cutting edges-filed of applications and limitations, *Ann CIRP*. 1991; 39: 413–25p.
6. Shaw M. The mechanism of chip formation with hard turning steel, *Ann CIRP*. 1998; 39: 77–82p.
7. Recht R. Adynamic analysis of high speed machining, *ASME Trans J Eng Ind*. 1985; 107: 309–15p.
8. Poulachon G., Moisan A., Jawahir I.S. Tool-wear mechanisms in hard turning with polycrystalline cubic boron nitride tools, *Wear*. 2001; 250: 576–86p.
9. Rtarya G., Choudhary S.K. State of the art in hard turning, *Int J Mach Tools Manuf.* 2012; 53: 1–14p.
10. Nakayama K. The formation of saw-toothed chip in metal cutting, *Proceedings of International Conference on Production Engineering.* Tokyo, Part 1, 1974, 572–7p.